Induction of Autophagy and Cell Death by Tamoxifen in Cultured Retinal Pigment Epithelial and Photoreceptor Cells

Kyung Sook Cho,[2,3] *Young Hee Yoon,*[1,3] *Jeong A. Choi,*[2] *Sook-Jeong Lee,*[2] *and Jae-Young Koh*[2]

Purpose. We investigated the mechanism of tamoxifen (TAM) retinotoxicity using human retinal pigment epithelial (RPE)-derived (ARPE-19) and photoreceptor-derived (661W) cells.

Methods. Cultured ARPE-19 and 661W cells were treated with 5 to 10 μM TAM, and the resultant cell death was quantified using lactate dehydrogenase (LDH) release assay. Cellular oxidative stress was determined by measuring 5-(and-6)-carboxy-2′,7′-dichlorohydrofluorescein diacetate (H_2-DCFDA) fluorescence. Changes in intracellular free zinc levels were monitored using the zinc-specific fluorescent dye, FluoZin-3 AM. Autophagic vacuole formation was assessed morphologically in ARPE-19 and 661W cells transfected with the fluorescent protein-conjugated markers, RFP-LC3 or GFP-LC3.

Results. Following exposure to TAM, both ARPE-19 and 661W cells had cytosolic vacuoles within 1 hour and underwent cell death within 18 hours. In both cell types, TAM-induced cell death was accompanied by increased oxidative stress and elevated zinc levels, and was attenuated by the antioxidant N-acetyl-L-cysteine (NAC) or the zinc chelator N,N,N′N′-tetrakis(-)(2-pyridylmethyl)-ethylenediamine (TPEN). The levels of LC3-II as well as the number of autophagic vacuoles (AVs) increased after TAM treatment. Double staining for lysosomes and AVs showed that autolysosome formation proceeded normally. Consistent with this, autophagy flux was increased. Finally, as shown in other cases of autophagic cell death, lysosomal membrane permeabilization (LMP) as well as caspase-dependent apoptosis contributed to TAM-induced cell death.

Conclusions. ARPE-19 and 661W cells were vulnerable similarly to TAM-induced cytotoxicity. Increases in zinc levels and oxidative stress, excessive activation of autophagy flux, and ultimately the occurrence of LMP and consequent caspase activation may contribute to the well-established retinal cytotoxicity of TAM. (*Invest Ophthalmol Vis Sci.* 2012; 53:5344–5353) DOI:10.1167/iovs.12-9827

From the [1]Department of Ophthalmology, NRL Neural Injury Research Center, and the [2]Department of Neurology, Asan Medical Center, University of Ulsan, College of Medicine, Seoul, Korea.

[3]These authors contributed equally to the work presented here and should therefore be regarded as equivalent authors.

Supported by grants from the National Research Foundation of Korea (NRF; 2005-0093836) and the Original Technology Research Program for Brain Science through NRF funded by the Ministry of Education, Science and Technology (2009-0081487).

Submitted for publication March 9, 2012; revised June 25, 2012; accepted July 3, 2012.

Disclosure: **K.S. Cho**, None; **Y.H. Yoon**, None; **J.A. Choi**, None; **S.-J. Lee**, None; **J.-Y. Koh**, None

Corresponding author: Jae-Young Koh, Department of Neurology & NRL Neural Injury Research Center, University of Ulsan College of Medicine, 388-1 Poongnap-Dong, Songpa-Gu, Seoul, Korea; jkko@amc.seoul.kr.

Tamoxifen (TAM) is a nonsteroidal estrogen receptor (ER) antagonist used widely as a chemotherapeutic agent against breast cancer.[1] However, in a subset of patients, TAM induces macula-involving retinopathy, which can compromise vision seriously,[2,3] especially in women treated with high daily or cumulative doses of TAM.[4] RPE generally has been considered the primary target of TAM-induced retinotoxicity.[5] However, recent clinical studies have reported that TAM also disrupts photoreceptors as well.[6–8]

The RPE is a single layer of cells adjacent to and surrounding the photoreceptor outer segment (POS) of the retina. As such, the RPE has critical roles in the maintenance of the POS, in part by removing shed debris of rods and cones.[9] On the other hand, photoreceptor cells are specialized type of neurons in the retina proper. The initial signal transduction for visual perception is the conversion of light energy to electrical signals in the outer segment of photoreceptor cells.[10] The finding that RPE and photoreceptors are damaged in TAM retinotoxicity may reflect RPE damage by TAM, since the RPE is necessary for the maintenance of overlying photoreceptors. Alternatively, TAM might well induce cytotoxicity to RPE and photoreceptors.

Because TAM is used increasingly to treat breast cancer patients, the prevalence and clinical significance of TAM-induced retinopathy also are rising. However, although it is known that TAM penetrates the blood-retinal barrier[11] and induces oxidative stress,[12] the mechanism of TAM-induced retinotoxicity is not yet clear. Because TAM is known to induce autophagy in certain cancer cells,[13] and since autophagy can cause cell death,[14] it seems possible that an autophagic mechanism also may be involved in TAM-induced retinopathy.

Autophagy or macroautophagy is a lysosome-dependent bulk degradation system for recycling of long-lived proteins, protein aggregates, and organelles, such as mitochondria, the endoplasmic reticulum, and peroxisomes.[15,16] It is activated under various cellular stress conditions, such as starvation and oxidative stress, and thus is essential for cellular viability. We have shown recently that TAM induces autophagic cell death in breast cancer cells independent of ERs.[14] Hence, it seems possible that TAM-induced retinopathy also may be caused by a similar mechanism.

In our study, we compared the vulnerability of human RPE-derived ARPE-19 cells and mouse photoreceptor-derived 661W cells to TAM toxicity. In addition, we examined the possibility that TAM-induced cell death occurs by an autophagic mechanism.

Materials and Methods

Cell Culture

ARPE-19 cells were obtained from the American Type Culture Collection (Cat #CRL-2302; Manassas, VA) and cultured in Dulbecco's Modified Eagle Medium Nutrient Mixture F-12 (DMEM/F-12; Invitrogen, Carlsbad, CA)

Investigative Ophthalmology & Visual Science, August 2012, Vol. 53, No. 9

supplemented with 10% fetal bovine serum (FBS; Invitrogen) and penicillin-streptomycin (100 IU/mL–100 μg/mL; Lonza, Allendale, NJ) at 37°C in a humidified 5% CO_2 incubator. The 661W cells were obtained from Muayyad R. Al-Ubaidi (University of Oklahoma, Oklahoma City, OK) and maintained in DMEM (Invitrogen) containing 10% FBS and penicillin-streptomycin. Cells were used after reaching approximately 80% confluence.

Drugs and Chemicals

TAM; N,N,N′N′-tetrakis(-)(2-pyridylmethyl)-ethylenediamine (TPEN); 3-methyladenine (3MA); and bafilomycin A1 (Baf A1) were purchased from Sigma (St. Louis, MO). N-acetyl-L-cysteine (NAC) was obtained from Merck Millipore (Calbiochem, Billerica, MA). ICI 182,780 was purchased from TOCRIS Bioscience (Bristol, UK). Hydrogen peroxide (H_2O_2) was purchased from Merck (Darmstadt, Germany). Pepstatin A was obtained from Biomol International (Plymouth Meeting, PA). Caspase-3 inhibitor (Z-D[OMe]-E[OMe]-V-D[OMe]-FMK; Z-DEVD-FMK) was purchased from R&D systems (Minneapolis, MN).

Assessment of Cell Death

TAM-induced cell death was quantified by measuring lactate dehydrogenase (LDH) activity released into the culture medium.[17] LDH activity was estimated using an automated microplate reader (UVmax; Molecular Devices, San Francisco, CA) by measuring the rate of decrease in absorbance at 340 nm. After subtraction of background (sham-washed control cultures), LDH values were normalized to the mean maximal value (defined as 100%) in parallel cultures exposed to 1 mM H_2O_2 for 18 hours, conditions that caused complete cell death.

Measurement of Reactive Oxygen Species (ROS) and Intracellular Zinc Level

The levels of intracellular ROS were measured using the fluorescent probe, 5-(and-6)-carboxy-2′,7′-dichlorohydrofluorescein diacetate (H_2-DCFDA), as described by the manufacturer (Molecular Probes, Eugene, OR). In brief, cells were incubated with 10 μM H_2-DCFDA for 15 minutes at 37°C and then washed in serum-free MEM (Invitrogen) without phenol red.

For measurement of intracellular zinc level, cells were stained with the zinc-specific fluorescent dye, 5 μM FluoZin-3AM (Invitrogen) for 30 minutes at 37°C, and then washed in serum-free MEM without phenol red. Cells were observed under a fluorescence microscope and photographed.

Plasmids

The GFP-LC3 plasmid was constructed as follows: Plasmid DNA containing the coding region of mouse microtubule-associated protein 1 light chain 3 (LC3; GenBank Accession No. NM_026160) inserted into *Sal*I and *Not*I sites in the pSPORT1 vector was purchased from the Korea Research Institute of Bioscience and Biotechnology (Daejeon, Korea). The LC3 coding region from this construct was digested with *Sal*I and *Bam*HI (Promega, Madison, WI) and subcloned into the corresponding sites of the pAcGFP1-C1 vector (Clontech, Mountain View, CA). The completed GFP-LC3 plasmid was verified by DNA sequencing. The GFP-LC3 construct was transfected into cells using Lipofectamine 2000 (Invitrogen), and its cellular expression was confirmed by Western blotting. The RFP-LC3 expression plasmid was a generous gift from Drs Maria Colombo and Michel Rabinovitch (Universidad Nacional de Cuyo, Mendoza, Argentina).

Live-Cell Confocal Microscopy

For live-cell imaging experiments, ARPE-19 cells were stained with 75 nM LysoTracker Green DND-26 and Red DND-99 (Invitrogen) in MEM for 5 to 30 minutes in a humidified CO_2 incubator, transferred to Hank's balanced salt solution (HBSS; Lonza), and observed under a confocal microscope at an excitation wavelength of 488 nm. Live-cell confocal images were obtained using an UltraView Confocal Imaging System (PerkinElmer, Waltham, MA) attached to a Nikon ECLIPSE TE2000 microscope (Melville, NY). All fluorescence intensities are expressed in arbitrary units.

Immunocytochemistry

Cells were fixed in 4% paraformaldehyde for 20 minutes at room temperature and permeabilized with 0.2% Triton X-100 containing 1% BSA in PBS for 15 minutes. After blocking with 1% BSA, fixed cells were incubated overnight at 4°C with primary antibody against cathepsin D (1:250 dilution; Santa Cruz Biotechnology, Santa Cruz, CA) and lysosomal-associated membrane protein-2 (LAMP-2, 1:1500 dilution; Developmental Studies Hybridoma Bank, Iowa City, IA). The stained cells were washed and incubated for 1 hour at room temperature with Alexa Fluor-conjugated secondary antibodies (Alexa Fluor 488-donkey anti-rabbit IgG; 1:500 dilution and Alexa Fluor 555-donkey anti-mouse IgG; 1:2000 dilution; Invitrogen). After incubating with secondary antibodies, cells were stained with the nuclear dye Hoechst 33342 (Invitrogen) in PBS for 2 minutes at room temperature. For negative controls, cultured cells were incubated with secondary antibody only.

Immunoblotting

After washing with serum-free medium, cells were suspended in lysis buffer (20 mM Tris-Cl pH 7.4, 150 mM NaCl, 1 mM EDTA, 1 mM EGTA, 1% Triton X-100, 2.5 mM sodium pyrophosphate, 1 μM Na_3VO_4, 1 μg/mL Leupeptin, 1 mM phenylmethylsulfonyl fluoride [PMSF)]) and centrifuged. Equal amounts of proteins were separated by SDS-PAGE on 10% or 12% polyacrylamide gels and transferred to polyvinylidene difluoride membranes (PVDF; Millipore, Bedford, MA). The membranes were blocked with 3% nonfat dried milk for 1 hour and incubated overnight at 4°C with anti-LC3 (1:1000 dilution; Novus, Littleton, CO) and anti-β-actin (1:5000 dilution; Sigma) antibodies, followed by incubation with horseradish peroxidase-conjugated goat anti-rabbit IgG (1:10,000 dilution; Pierce, Woodstock, IL). For p62 immunoblotting, treatment with anti-p62 (1:500 dilution; Santa Cruz Biotechnology) antibody was followed by treatment with horseradish peroxidase-conjugated goat anti-mouse IgG (1:10,000 dilution; Pierce). Immunoreactive proteins were visualized using a chemiluminescence substrate (Millipore) and analyzed quantitatively by densitometry using ImageJ Software (Bethesda, MD). All experiments were performed in at least triplicate.

Immunoblotting for Cathepsin D in Lysosomes or the Cytosol

For preparation of the released cathepsin D from lysosomes to the cytosol, we extracted cytosolic proteins using digitonin (Sigma). In brief, cytosolic proteins were extracted with extraction buffer (250 mM sucrose, 20 mM HEPES, 10 mM KCl, 1.5 mM $MgCl_2$, 1 mM EDTA, and 1 mM EGTA) containing 25 μg/mL digitonin by rocking (100 revolutions per minute) on ice for 15 minutes. Protein in cytosolic extracts was precipitated with 10% trichloroacetic (TCA), washed with methanol, and lysed with lysis buffer (20 mM Tris-Cl pH 7.4, 150 mM NaCl, 1 mM EDTA, 1 mM EGTA, 1% Triton X-100, 2.5 mM sodium pyrophosphate, 1 μM Na_3VO_4, 1 μg/mL Leupeptin, 1 mM PMSF). Equal amounts of proteins were separated by SDS-PAGE and analyzed by immunoblotting using antibodies against cathepsin D (Santa Cruz Biotechnology), LAMP-2 (1:5000 dilution; Developmental Studies Hybridoma Bank) and α-Tubulin (Cell Signaling, Boston, MA), as described above.

Transmission Electron Microscopy

ARPE-19 cells were exposed to TAM for 1 and 6 hours, and then harvested with PBS. The cells were fixed in 2.5% glutaraldehyde in 0.1 M phosphate buffer solution. Ultrathin sections of cell pellets were cut,

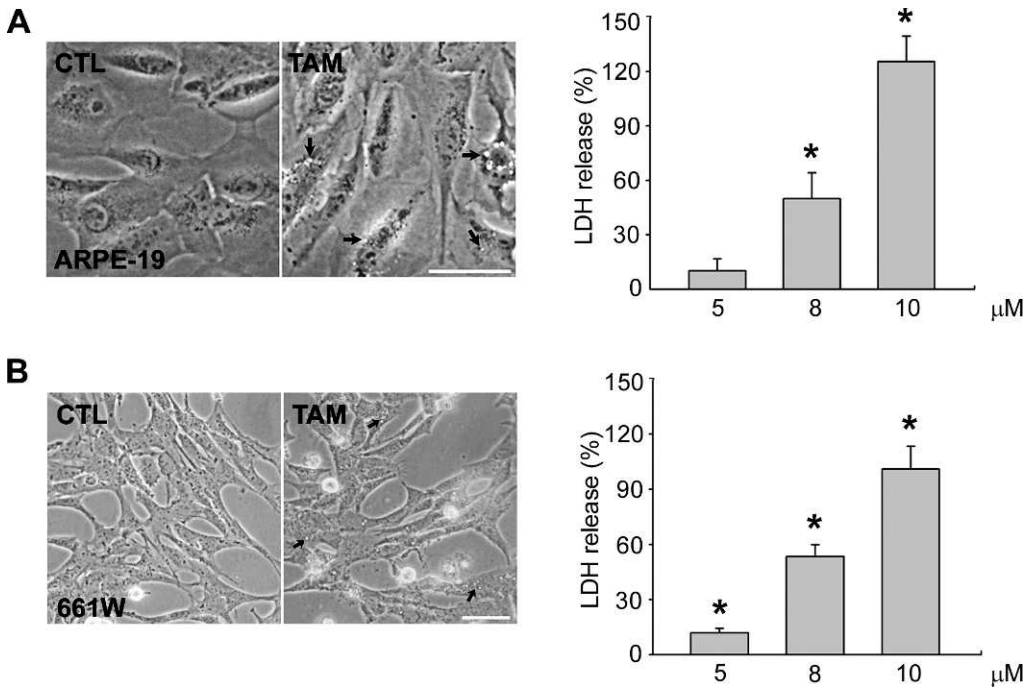

Figure 1. TAM induces cell death and vacuole formation in ARPE-19 and 661W cells. Phase-contrast photomicrographs of ARPE-19 (**A**) and 661W (**B**) cells, sham-washed (CTL) or treated with TAM for 3 hours. Small dots and vacuoles were formed in both cell types treated with TAM. Scale bar: 50 μm. LDH activity, expressed as mean ± SEM, was measured in the medium of ARPE-19 (**A**) and 661W (**B**) cells exposed to the indicated concentrations of TAM for 18 hours (*$P < 0.05$ compared to controls; $n = 3$ cultures).

prepared, photographed under an electron microscope (1200EX-II; JEOL, Tokyo, Japan).

Statistics

All data are presented as means ± SEM. Student's *t*-tests were used to analyze differences between two groups. Multiple sets of data were compared using one-way ANOVAs followed by Fisher LSD post hoc tests. Values of $P < 0.05$ were considered statistically significant.

Results

TAM-Induced Vacuole Formation and Cell Death in ARPE-19 and 661W Cells

To investigate the cytotoxicity of TAM, we exposed human RPE-derived ARPE-19 cells and photoreceptor-derived 661W cells to different concentrations (5–10 μM) of TAM. Within 3 hours of exposure to 8 μM TAM, the majority of cells of both cell types had fine vacuoles in their cytosol (Figs. 1A, 1B). After 18 hours, most cells exhibited signs of cell death, such as swollen cell bodies and detachment from the bottom of culture vessels. Cell death was confirmed by trypan blue staining, and quantified using LDH-release assays (Figs. 1A, 1B). In both cell types, 5 μM TAM induced virtually no cell death, whereas 10 μM killed almost all cells. At a concentration of 8 μM, TAM induced approximately 50% to 60% cell death. The vulnerability to TAM-induced cytotoxicity was not significantly different between the two cell types.

Increased Oxidative Stress and Cytosolic Free-Zinc Levels in TAM-Treated Cells

Previous studies have reported that TAM increases the level of ROS in breast cancer cells.[18] Hence, we examined the possibility that oxidative stress contributes to TAM-induced cell death in RPE- and photoreceptor-derived cells. Levels of DCF fluorescence, an indicator of ROS, were increased markedly in ARPE-19 and 661W cells after exposure to 8 μM TAM (Figs. 2A, 2E). Consistent with a role for ROS in TAM-induced retinotoxicity, addition of the antioxidant, NAC, substantially attenuated TAM-induced cell death in both cell types (Figs. 2C, 2D, 2G, 2H).

Our previous studies have demonstrated that zinc dyshomeostasis has a key role in several cases of oxidative cell injury.[19,20] To examine whether zinc dyshomeostasis also occurs in association with TAM-induced toxicity in ARPE-19 and 661W cells, we used the zinc-specific fluorescent dye, FluoZin-3, to follow changes in cytosolic free-zinc levels. Within 1 hour of exposure, ARPE-19 and 661W cells exhibited increases in cytosolic zinc fluorescence (Figs. 2B, 2F), suggesting that zinc dyshomeostasis contributes to TAM-induced oxidative stress. Consistent with this interpretation, chelation of zinc with TPEN largely eliminated the increases in DCF fluorescence and cell death induced by TAM.

Increased LC3-II Levels in ARPE-19 and 661W Cells

TAM is known to activate autophagy in breast cancer and colorectal cancer cells.[13,21,22] In addition, we have shown that an autophagic mechanism contributes to TAM-induced death of breast cancer cells.[18] Western blots revealed that TAM treatment increased the levels of LC3-II, a marker for autophagy, in ARPE-19 and 661W cells (Figs. 3A, 3E). These results were confirmed using cells transfected with red or green fluorescent protein-conjugated LC3 (RFP-LC3 and GFP-LC3, respectively), which showed that TAM treatment increased LC3 (+) autophagic vacuole formation (Figs. 3B, 3F). Moreover, transmission electron microscopic images showed that double-membrane autophagic vacuoles accumulated in ARPE-19 cells (Fig. 3C). Finally, consistent with the contribution of autophagy to TAM-induced cell death, 3MA, which blocks autophagy activation (including LC3-II conver-

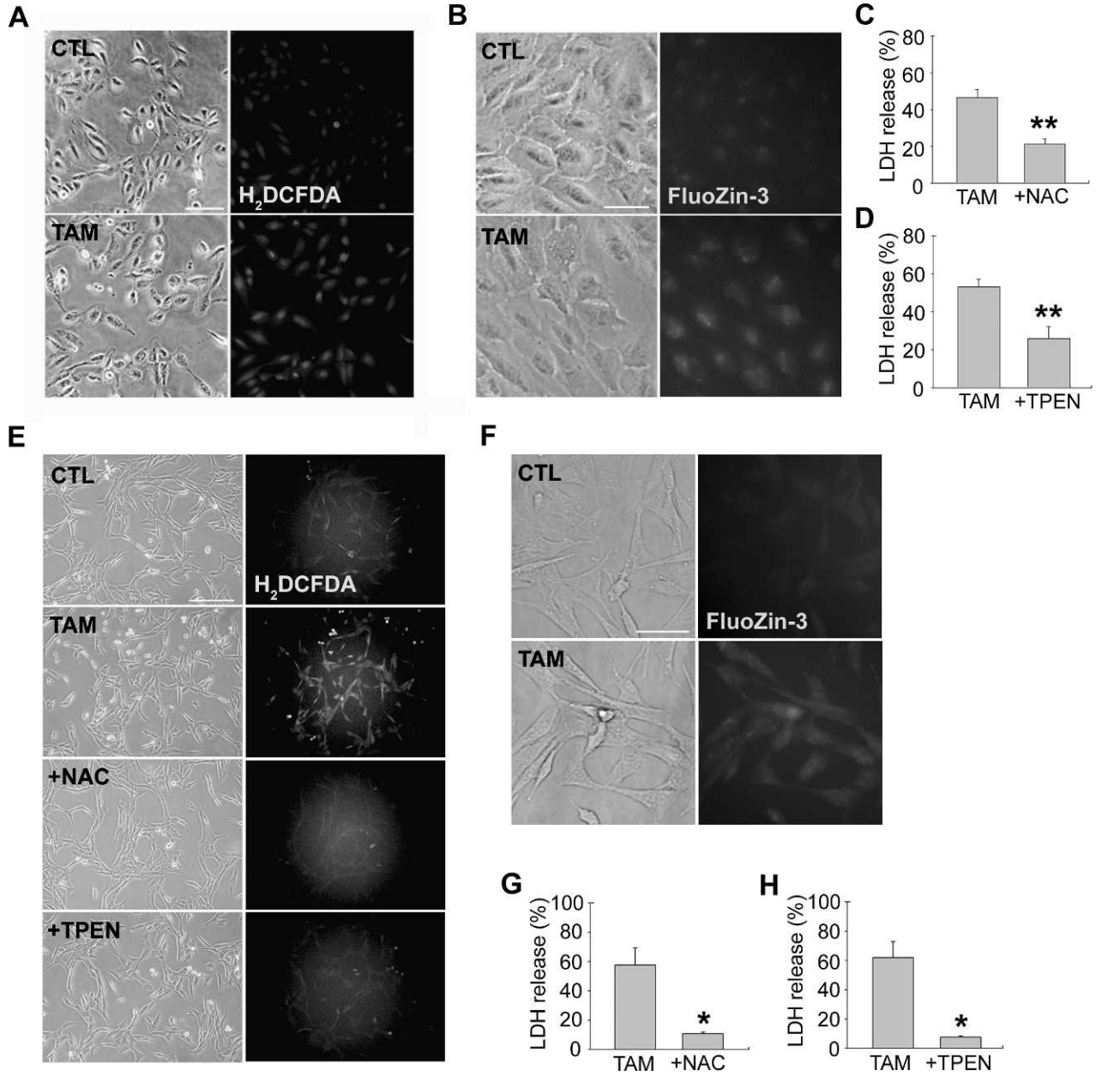

Figure 2. TAM induces oxidative injury to ARPE-19 and 661W cells in a zinc-dependent manner. (**A**) Phase-contrast and fluorescence photomicrographs of ARPE-19 cells stained with H_2-DCFDA. DCF fluorescence increased after 12 hours of exposure to 8 μM TAM alone, indicating that TAM increased ROS levels in ARPE-19 cells. Scale bar: 100 μm. (**B**) Phase-contrast and FluoZin-3 fluorescence photomicrographs of sham-washed control and TAM (8 μM)-treated ARPE-19 cells. Zinc levels were increased by TAM. Scale bar: 50 μm. (**C**) *Bars* represent LDH release (means ± SEM) in ARPE-19 cells after treatment with TAM alone (8 μM, 18 hours) or TAM plus 1 mM NAC. TAM-induced cell death was attenuated by NAC (**$P < 0.01$, compared to TAM alone; $n = 3$). (**D**) *Bars* represent LDH release (means ± SEM) in ARPE-19 cell cultures treated with TAM alone (8 μM, 18 hours) or TAM plus 0.25 μM TPEN (**$P < 0.01$, compared to TAM alone; $n = 3$). (**E**) Phase-contrast and fluorescence photomicrographs of 661W cells stained with H_2-DCFDA. DCF fluorescence increased after 12 hours of exposure to 8 μM TAM alone. TAM-induced oxidative stress was reduced markedly by NAC and TPEN. Scale bar: 200 μm. (**F**) Phase-contrast and FluoZin-3 fluorescence photomicrographs of sham-washed (control) and TAM (8 μM)-treated 661W cells. Zinc levels were increased by TAM. Scale bar: 50 μm. (**G**) *Bars* denote LDH release (means ± SEM) in 661W cell cultures treated with TAM alone (8 μM, 18 hours) or TAM plus 1 mM NAC. TAM-induced cell death was reduced significantly by NAC (*$P < 0.05$, compared to TAM alone; $n = 3$). (**H**) *Bars* represent LDH release (means ± SEM) in 661W cell cultures treated with TAM alone (8 μM, 18 hours) or TAM plus 0.25 μM TPEN. TPEN attenuated TAM-induced cell death. (*$P < 0.05$, compared to TAM alone; $n = 3$).

sion), and bafilomycin A1, which blocks autophagy flux, markedly reduced cell death (Figs. 3D, 3G, 3H).

Increased Autophagy Flux in TAM-Treated Cells

For autophagy to be completed, the fusion between autophagosomes and lysosomes, that is, the formation of autolysosomes, is essential.[23] If this step is inhibited, autophagy flux is disrupted, but the level of LC3-II and the number of autophagosomes still can increase. To determine whether TAM-induced LC3-II conversion and autophagosome formation were due to the failure of autophagolysosome formation, as is the case with chloroquine,[24] we stained RFP-LC3-transfected ARPE-19 cells and GFP-LC3-transfected 661W cells with

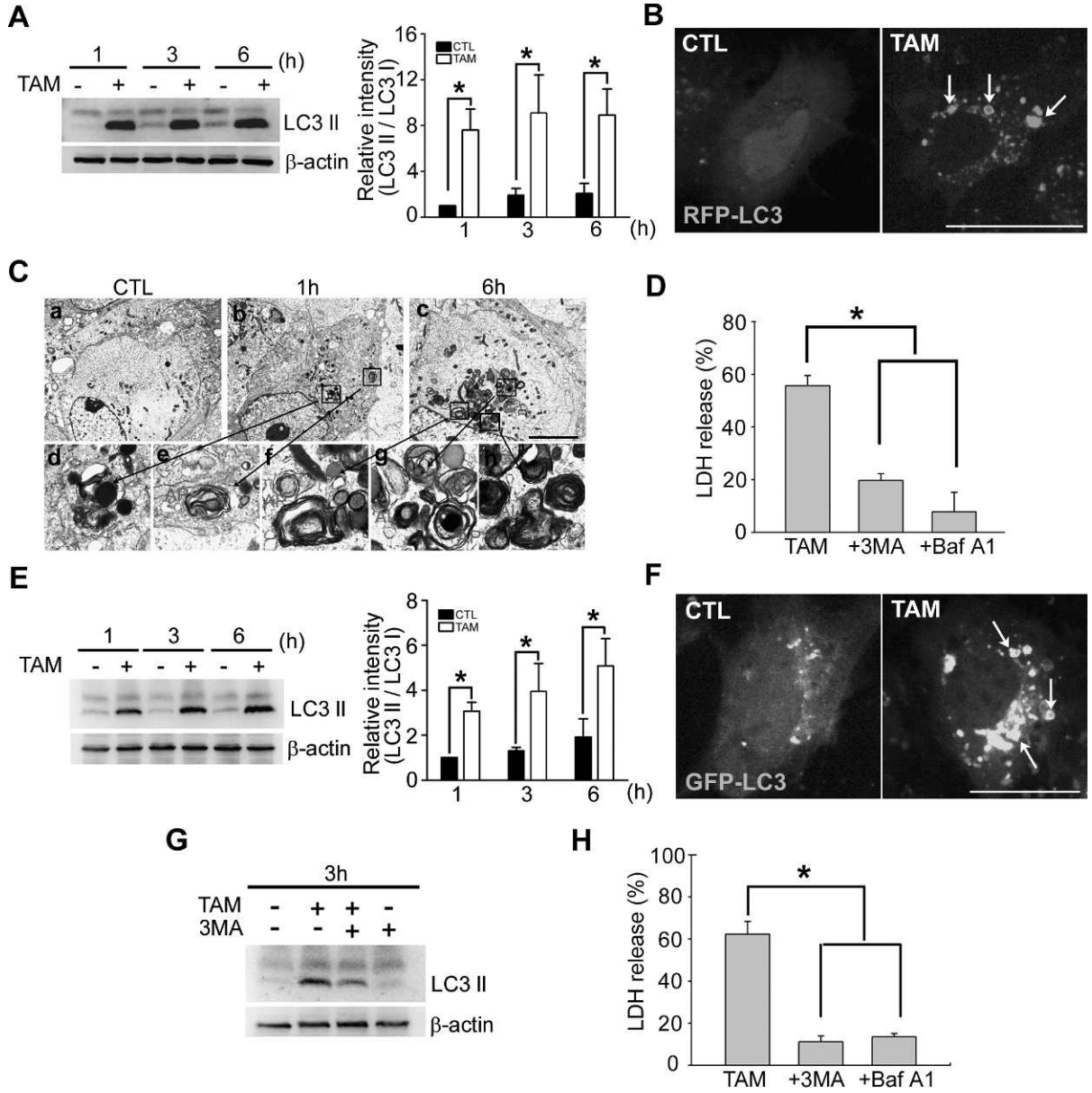

Figure 3. TAM induces autophagy in ARPE-19 cells and 661W cells. (**A**) Immunoblots for LC3 in samples taken at the indicated times from sham-washed control and TAM (8 μM)-treated ARPE-19 cells. *Bars* denote fold increases in densitometric values of the LC3-II band, normalized to the density of the corresponding LC3-I band and expressed as mean ± SEM (*$P < 0.05$; $n = 3$). (**B**) Live-cell confocal microscopic images of RFP-LC3-transfected ARPE-19 cells, sham-washed or after 6 hours of exposure to 8 μM TAM. TAM treatment significantly increased RFP-LC3 (+) autophagic vacuoles (*arrows*). Scale bar: 10 μm. (**C**) Transmission electron microscopy (TEM) of ARPE-19 cells under control conditions (sham washed; [**a**] and after 1 hour (**b**) or 6 hours (**c**) treatment with 8 μM TAM. Enlarged images ([**d**, **e**], 1 hour; [**f**–**h**], 6 hours) show autophagosomes (double- or multiple-membrane vacuoles containing cytoplasmic material and organelles). Scale bar: 5 μm. (**D**) *Bars* denote LDH release (means ± SEM) in ARPE-19 cell cultures treated with TAM (8 μM, 18 hours) alone, TAM plus 2.5 mM 3MA, or TAM plus 10 nM Baf A1 (*$P < 0.05$, compared to TAM alone; $n = 3$). (**E**) Western blot analysis for LC3 in samples prepared from 661W cells, sham-washed or treated for 6 hours with 8 μM TAM. *Bars* denote fold increases in densitometric values of the LC3-II band, normalized to the density of the corresponding LC3-I band and expressed as mean ± SEM (*$P < 0.05$; $n = 3$). (**F**) Live-cell confocal microscopic images of GFP-LC3-transfected 661W cells, sham-washed or exposed to 8 μM TAM for 6 hours. Scale bar: 10 μm. (**G**) Western blot analysis for LC3 in samples prepared from 661W cells, sham-washed or treated for 3 hours with 8 μM TAM alone, TAM plus 2.5 mM 3MA, or 3MA alone. (**H**) *Bars* represent LDH release (means ± SEM) in 661W cell cultures treated with TAM (8 μM, 18 hours) alone, TAM plus 2.5 mM 3MA, or TAM plus 10 nM Baf A1 (*$P < 0.05$, compared to TAM alone; $n = 5$).

LysoTracker-Red and LysoTracker-Green, respectively, and observed them with live-cell confocal microscopy. In TAM-treated cells, LC3 and lysosomal signals overlapped substantially (Figs. 4A, 4B), indicating that autophagosomes fused successfully with lysosomes. In addition, an autophagy flux assay using the vacuolar H^+-ATPase (V-ATPase) inhibitor Baf A1 showed that TAM indeed increased autophagy flux (Fig. 4C).[25]

In addition, levels of p62, a functional indicator of autophagic degradation,[26] were measured following TAM treatment. p62 levels were reduced substantially after TAM treatment, consistent with upregulated autophagy (Fig. 4D). As expected, Baf A1 not only blocked the TAM-induced reduction of p62, but also increased significantly the basal level of it, indicating that p62 is degraded constantly via autophagy.

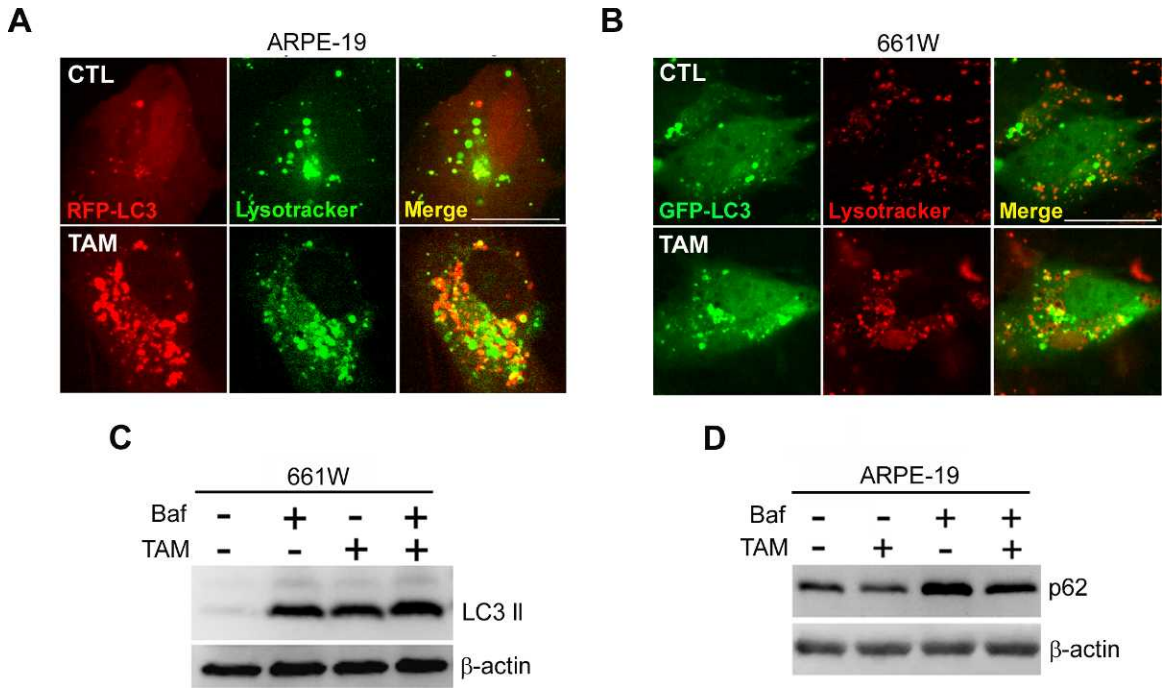

Figure 4. TAM increases autophagy flux. (**A**, **B**) Live-cell confocal images of RFP-LC3 (ARPE-19) and GFP-LC3 (661W) transfected cells stained with LysoTracker-Green or -Red. Cultures were sham-washed or exposed to 8 μM TAM for 6 hours. In both cell types, the majority of LC3 (+) autophagosomes were autolysosomes. Scale bar: 10 μm. (**C**) Immunoblots for LC3 in samples prepared from 661W cells, sham-washed or treated for 3 hours with 0.2 μM Baf A1 (Baf) alone, 8 μM TAM alone, or Baf plus TAM. The finding that addition of Baf further increased LC3-II levels compared to TAM alone is consistent with an increase in autophagy flux. (**D**) Western blots for p62 in samples prepared from ARPE-19 cells, sham-washed or treated for 3 hours with 8 μM TAM alone, 0.2 μM Baf alone, or TAM plus Baf A1. Again, the finding that addition of Baf further increased LC3-II levels compared to TAM alone is consistent with an increase in autophagy flux.

Attenuation of TAM-Induced Autophagy by an Antioxidant or a Zinc Chelator

Oxidative stress and increases in cytosolic zinc levels have been implicated as triggers of autophagy in certain cell types. Because TAM increased the levels of ROS as well as free zinc in ARPE-19 and 661W cells, we investigated whether these changes were linked causally to autophagy activation by TAM. As noted above, treatment with TAM induced autophagic vacuoles. Addition of either NAC or TPEN reduced TAM-induced vacuole formation substantially (Fig. 5A). Moreover, Western blot analyses revealed that the increases in LC3-II levels induced by TAM were attenuated by the addition of NAC or TPEN (Figs. 5B, 5C). These results indicated that TAM-induced autophagy is caused, at least in part, by increases in ROS and cytosolic zinc.

Lysosomal Membrane Permeabilization (LMP) in TAM-Induced Autophagic Cell Death

Whereas autophagy has been recognized as an important mechanism for cell survival, a number of studies have demonstrated that excessive autophagy can lead to cell death. We demonstrated that, in hippocampal neurons and astrocytes, oxidative stress induces autophagy-dependent cell death, in which LMP has a key role.[19,20] Hence, we investigated whether LMP has a role in TAM-induced cell death.

ARPE-19 cells were co-immunostained for cathepsin D, a lysosomal enzyme, and LAMP-2. Whereas control cells showed a particulate pattern of cathepsin D immunoreactivity that overlapped substantially with LAMP-2 immunoreactivity, TAM-treated cells exhibited a more diffuse pattern of cathepsin D immunoreactivity dissociated from LAMP-2 immunoreactivity (Fig. 6A). These changes were blocked completely by addition of NAC or TPEN (Fig. 6D), and attenuated effectively by addition of pepstatin A, an inhibitor of cathepsin D, indicating that LMP contributes to TAM-induced cell death (Fig. 6C). In addition, using immunoblotting we confirmed increases in the cytosolic level of cathepsin D (Fig. 6B).

Independence of TAM-Induced Autophagy upon ER Activation

Finally, we examined whether TAM-induced autophagy in ARPE-19 or 661W cells was ER-dependent. We demonstrated that TAM-induced autophagy in breast cancer cells is not dependent on ERs. Two lines of evidence suggest that this also is the case in ARPE-19 and 661W cells. First, light microscopic examinations showed that vacuole formation, a morphologic indicator of autophagy, was not altered by the addition of the potent and specific ER inhibitor, ICI 182,780 (Fig. 6E). Second, Western blots revealed that ICI 182,780 failed to inhibit TAM-induced increases in LC3-II levels (Fig. 6F).

The Role of Caspase-Dependent Apoptosis in TAM-Induced Cell Death

We examined whether a caspase-dependent mechanism contributed to TAM-induced cell death in RPE and 661W cells. In both cases, we found that DEVD, a caspase-3-seletive inhibitor, significantly attenuated TAM-induced cell death. Since 3MA also blocked the cell death (Fig. 7A), but on the other hand, LC3-II levels were not attenuated by DEVD (Fig. 7B), it is likely that excessive autophagy is an upstream event of caspase activation in this case.

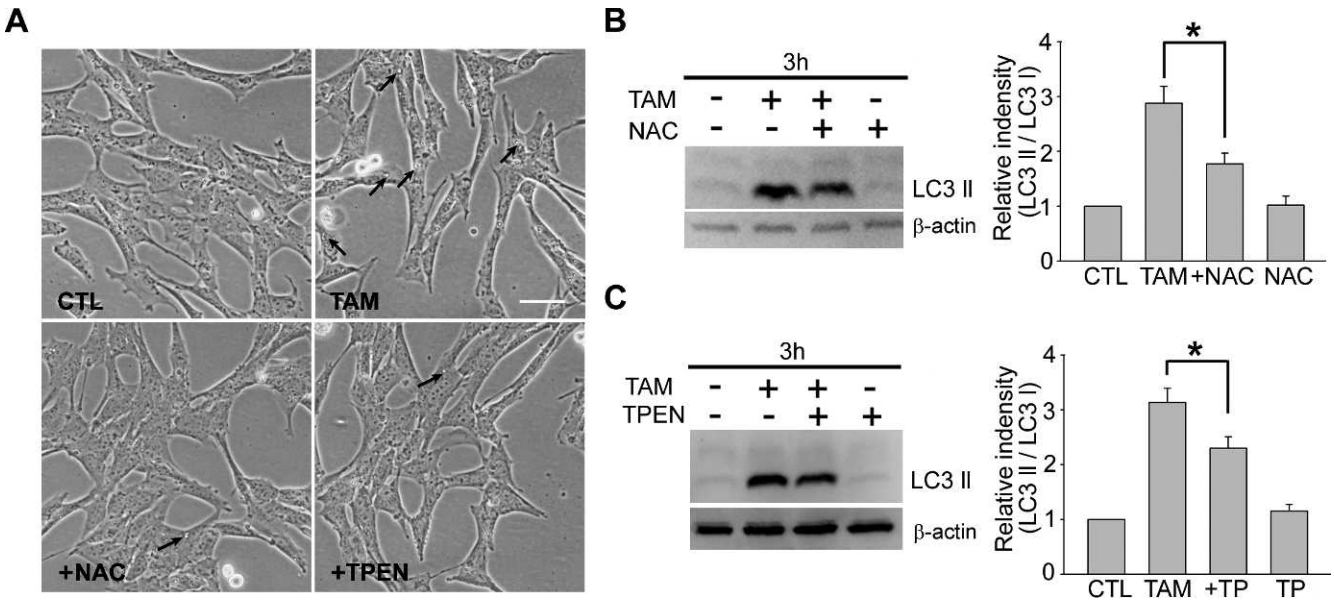

Figure 5. TAM-induced autophagy is dependent on ROS and zinc. (**A**) Phase-contrast photomicrographs of 661W cells, sham-washed or treated for 6 hours with 8 μM TAM, TAM plus 1 mM NAC, or TAM plus 0.25 μM TPEN. TAM-induced vacuole formation (*arrows*) was inhibited by NAC and TPEN. Scale bar: 50 μm. (**B**) Western blots for LC3 in samples prepared from 661W cells, sham-washed or treated for 3 hours with 8 μM TAM alone, TAM plus 1 mM NAC, or NAC alone. *Bars* denote fold increases in densitometric values of the LC3-II bands, normalized to those of the corresponding LC3-I bands and expressed as mean ± SEM (*$P < 0.05$; $n = 4$). (**C**) Western blots for LC3 in samples prepared from 661W cells, sham-washed or treated for 3 hours with 8 μM TAM alone, TAM plus 0.25 μM TPEN, or TPEN alone. *Bars* denote fold increases in densitometric values of the LC3-II bands, normalized to the density of the corresponding LC3-I band and expressed as mean ± SEM (*$P < 0.05$; $n = 8$).

Induction of Autophagy by Nontoxic Concentrations of TAM

Since autophagy also is known to have cytoprotective effects,[27–29] we tested whether nontoxic concentrations (0.1–5 μM) of TAM may be effective in activating autophagy. Whereas 0.1 and 1 μM TAM was not effective, 5 μM TAM that was not cytotoxic (Fig. 1) activated autophagy significantly (Fig. 7C). Hence, it seems possible that nontoxic concentrations of TAM, may be cytoprotective in certain cases.

Discussion

One of the central findings of our study is that TAM induced functional autophagy in human RPE- and photoreceptor-derived (661W) cells in culture. Reduced autophagy may be linked causally to degenerative conditions, such as age-related macular degeneration,[30,31] suggesting the potential of TAM as a treatment for these conditions. In fact, TAM has shown promising therapeutic effects[32] in patients with amyotrophic lateral sclerosis, in which abnormal autophagy is implicated.[33]

Despite these potentially beneficial effects, at high concentrations, TAM clearly was toxic to ARPE and 661W cells. Notably, there was no difference between ARPE-19 cells and 661W cells in terms of vulnerability to TAM cytotoxicity. If the cytotoxic effects of TAM observed here were to be extended to an in vivo setting, TAM would be predicted to injure RPE cells and photoreceptor cells at the same time, consistent with recent findings.[7,34,35] Demonstrating this convincingly may require further studies using animal models. Of note, the LC_{50} of TAM against MCF-7 breast cancer cells was reported to be approximately 17 μM, which is twice as high as that for ARPE-19 and 661W cells. Hence, at least in culture conditions, retinal cells appear to be even more vulnerable to TAM toxicity than breast cancer cells, which are the primary target of TAM chemotherapy. This might explain why the retina is a frequently involved tissue in TAM side effects.

Our results demonstrated that excessive autophagy also is an underlying mechanism in the acute toxicity paradigm. 3MA, which blocks the initiating event of autophagy, greatly reduced TAM cytotoxicity in both retinal cell types. Moreover, Baf A1, which blocks autophagy flux by inhibiting the fusion of autophagosomes and lysosomes, also was effective in reducing TAM cytotoxicity. The involvement of autophagy in cell death is not surprising, given that similar findings have been observed in diverse cell types.[14,36–38] As in all cases of key regulators of cell biology, deficiency and excess can be detrimental to cell survival.

Intriguingly, TAM induced autophagy and autophagic cell death appeared to be independent of ERs. Although the actual molecular mechanism underlying autophagy induction by TAM currently is unclear, interactions between oxidative stress and zinc dyshomeostasis are likely important upstream events.

An increasing body of evidence supports the role of cellular zinc dyshomeostasis in autophagy, oxidative stress, and cell death.[39,40] Oxidative stress can release free zinc from zinc-binding proteins, such as metallothioneins; conversely, increases in free-zinc levels can potentiate oxidative stress via activation of protein kinase C and NADPH oxidase. Free zinc accumulates concurrently in mitochondria and lysosomes.[41–43] Zinc accumulation in mitochondria disrupts oxidative phosphorylation, resulting in ROS generation. On the other hand, zinc chelation with TPEN dramatically reduces autophagosome formation, suggesting the involvement of zinc in the initiation of autophagy. The site of zinc action in autophagy, however, is not known. What is of interest is that free zinc accumulates in autophagosomes, including autolysosomes. Hence, zinc may have positive roles in the autophagy pathway. However, as we have shown,[14] too much zinc in lysosomes, especially in combination with oxidative stress, can result in LMP. In the present culture conditions, TAM also induced LMP. Moreover, addition of pepstatin A attenuated cell death, indicating that

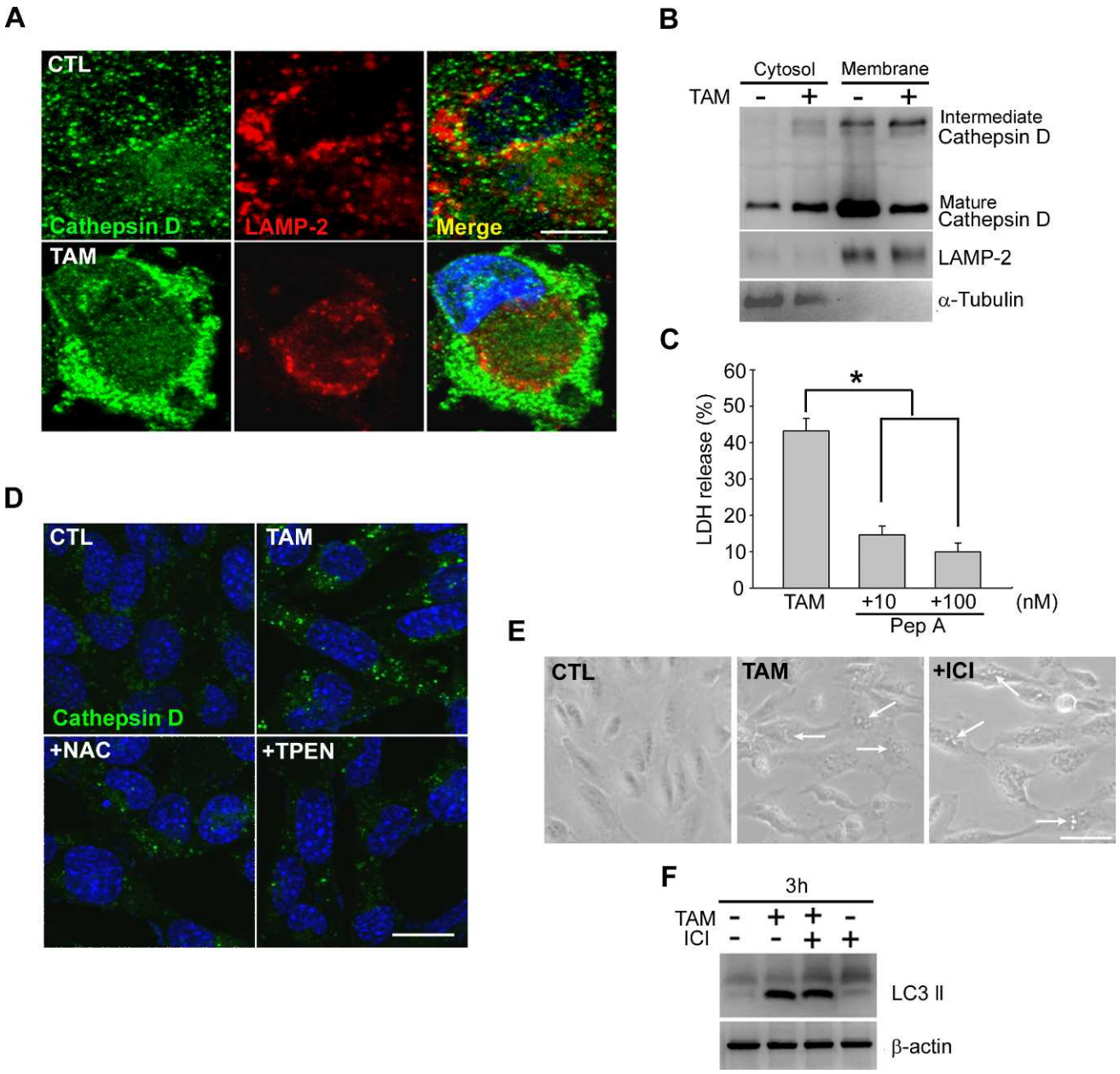

Figure 6. TAM-induced autophagic cell death is accompanied by LMP and is independent of ERs. (**A**) Fluorescence photomicrographs of ARPE-19 cells, sham-washed (CTL) or treated for 12 hours with TAM, then immunostained with anti-cathepsin D and LAMP-2 antibodies. Whereas immunoreactivities for cathepsin D and LAMP-2 were overlapped substantially in control (CTL) cells, in TAM-treated cells, cathepsin D immunoreactivity appeared in the cytosol, separately from that of LAMP-2, consistent with LMP. Scale bar: 10 μm. (**B**) Immunoblotting for cathepsin D in cytosolic fractions and pellets in samples prepared from ARPE-19 cells. Immunoblots for α-tubulin and LAMP-2 were checked to see whether samples were well fractionated. Levels of intermediate and mature forms of cathepsin D increased in the cytosol after exposed to 8 μM TAM for 12 hours. At the same time, the level of mature cathepsin D was reduced significantly in TAM-treated cells. (**C**) Bars represent LDH release (means ± SEM) in ARPE-19 cells treated with TAM (8 μM, 18 hours) alone or with TAM plus 0.01 or 0.1 μM pepstatin A (Pep A; $^*P < 0.05$, compared to TAM alone; $n = 3$). (**D**) Fluorescence photomicrographs of 661W cells immunostained with anti-cathepsin D antibody. Cells were sham-washed or treated for 6 hours with TAM alone, TAM plus NAC, or TAM plus TPEN. Scale bar: 20 μm. (**E**) Phase-contrast photomicrographs of ARPE-19 cells, sham-washed or treated for 12 hours with 8 μM TAM or TAM plus ICI 182,780 (ICI). ICI had no effect on TAM-induced vacuole formation. Scale bar: 50 μm. (**F**) Immunoblots for LC3 in samples prepared from 661W cells, sham-washed or treated for 3 hours with 8 μM TAM alone, TAM plus 1 μM ICI, or ICI alone.

LMP contributes to TAM-induced cell death. This finding is consistent with other accounts of autophagic cell death.

LMP can induce cell death by diverse mechanisms, including caspase-dependent apoptosis.[44–47] Also in case of TAM-induced death of ARPE-19 and 661W cells, a caspase-3-specific inhibitor DEVD attenuated cell death, indicating the contribution by caspase. Since 3MA also blocked the cell death, but LC3-II levels were not attenuated by DEVD, it is likely that excessive autophagy is an upstream event of caspase activation in this case. Similar caspase-dependent cell death was reported in the autophagic death of U937 human leukemic cells by tetraarsenic hexoxide, and rat astrocyte by aluminum maltolate and human colon carcinoma cell line HTC116 by 11′-deoxyverticillin A (C42).[48–51]

In conclusion, we found that TAM, a widely used anti-ER chemotherapeutic agent, is toxic to retinal RPE-derived (ARPE-

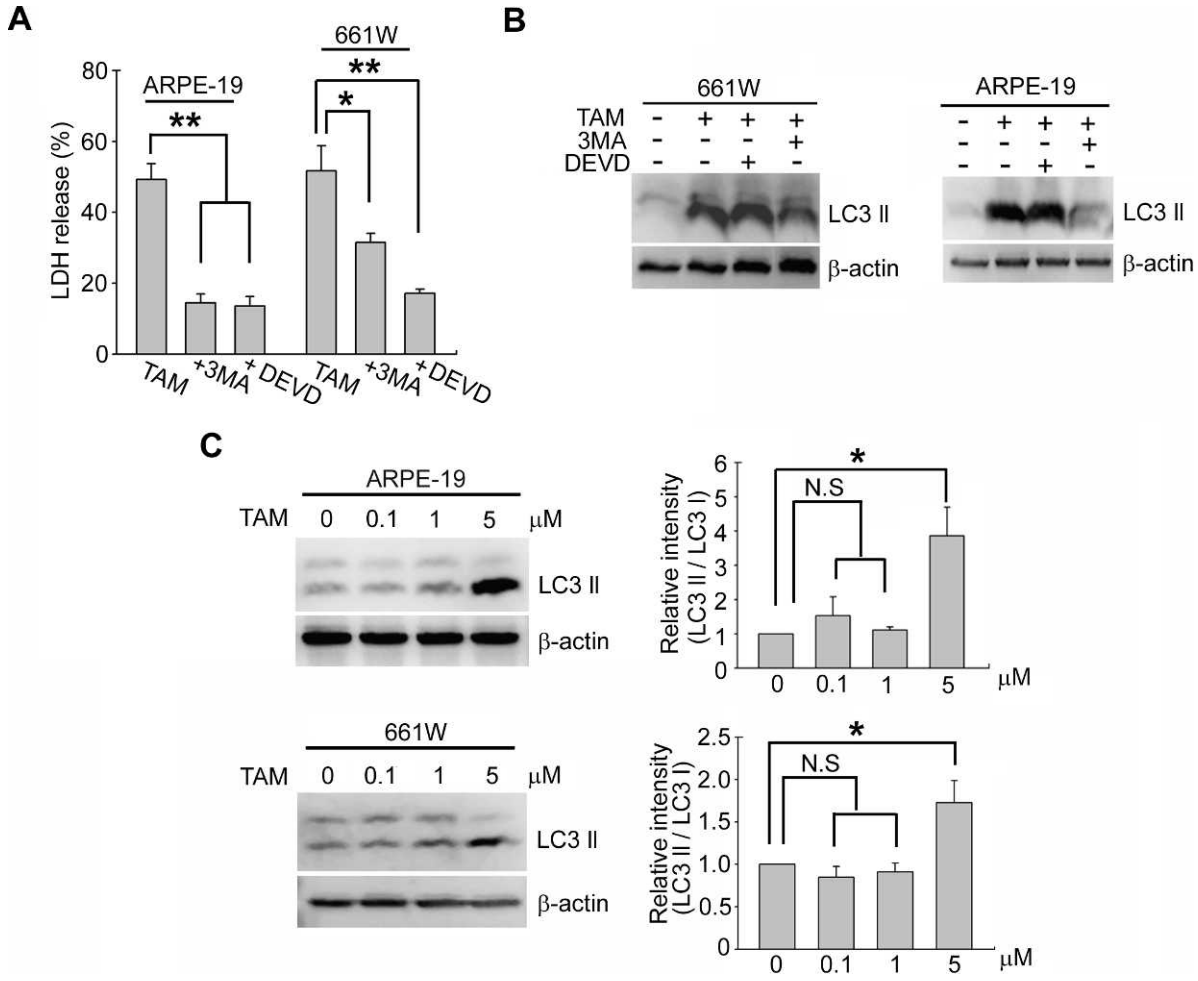

Figure 7. TAM-induced autophagic cell death is accompanied by caspase-dependent apoptosis. (**A**) *Bars* represent LDH release (means ± SEM) in ARPE-19 and 661W cell cultures treated with TAM alone (8 μM, 18 hours) or TAM plus 2.5 mM 3MA, or TAM plus 1 μM DEVD. DEVD significantly attenuated TAM-induced cell death (*$P < 0.05$ and **$P < 0.01$, compared to TAM alone; $n = 3$). (**B**) Immunoblots for LC3 in samples prepared from in ARPE-19 and 661W cell cultures, sham-washed or treated for 3 hours with 8 μM TAM alone, TAM plus 1 μM DEVD, or TAM plus 2.5 mM 3MA. Increases in LC3-II level were inhibited by 3MA, but not altered by DEVD. (**C**) Western blot for LC3 in samples taken from ARPE-19 or 661W cells treated for 1 hour with sham wash only or 0.1, 1, and 5 μM TAM. *Bars* denote fold increases in densitometric values of the LC3-II band, normalized to the density of the corresponding LC3-I band expressed as mean ± SEM (*$P < 0.05$; $n = 3$).

19) and photoreceptor-derived (661W) cells, but it acts in an ER-independent manner. In this latter context, the mechanistic link between TAM and these events should be investigated further to enhance our understanding of TAM pharmacology. If the ER-dependent anticancer effects of TAM can be separated from its ER-independent cytotoxic effects, it may be possible to develop a more efficient drug with fewer retinal side effects. Another salient point of our study is that TAM is a potent and effective inducer of functional autophagy in retinal cells. Again, if the side effects of TAM can be managed properly, this pharmacologic action of TAM could be used in various degenerative conditions in which deficient autophagy has been implicated as a pathogenic mechanism. In this regard, it is of note that 5 μM TAM that does not induce cell death still significantly activates autophagy.

References

1. Jensen EV, Jordan VC. The estrogen receptor: a model for molecular medicine. *Clin Cancer Res*. 2003;9:1980–1989.
2. Paganini-Hill A, Clark LJ. Preliminary assessment of cognitive function in breast cancer patients treated with tamoxifen. *Breast Cancer Res Treat*. 2000;64:165–176.
3. Sadowski B, Kriegbaum C, Apfelstedt-Sylla E. Tamoxifen side effects, age-related macular degeneration (AMD) or cancer associated retinopathy (CAR)? *Eur J Ophthalmol*. 2001;11:309–312.
4. Ah-Song R, Sasco AJ. Tamoxifen and ocular toxicity. *Cancer Detect Prev*. 1997;21:522–531.
5. Engelke M, Tykhonova S, Zorn-Kruppa M, Diehl H. Tamoxifen induces changes in the lipid composition of the retinal pigment epithelium cell line D407. *Pharmacol Toxicol*. 2002;91:13–21.
6. Baget-Bernaldiz M, Soler Lluis N, Romero-Aroca P, Traveset-Maeso A. Optical coherence tomography study in tamoxifen maculopathy. *Arch Soc Esp Oftalmol*. 2008;83:615–618.
7. Gualino V, Cohen SY, Delyfer MN, Sahel JA, Gaudric A. Optical coherence tomography findings in tamoxifen retinopathy. *Amer J Ophthalmol*. 2005;140:757–758.
8. Ko TH, Fujimoto JG, Duker JS, et al. Comparison of ultrahigh- and standard-resolution optical coherence tomography for imaging macular hole pathology and repair. *Ophthalmology*. 2004;111:2033–2043.
9. Bosch E, Horwitz J, Bok D. Phagocytosis of outer segments by retinal pigment epithelium: phagosome-lysosome interaction. *J Histochem Cytochem*. 1993;41:253–263.

10. Bok D. Retinal photoreceptor-pigment epithelium interactions. Friedenwald lecture. *Invest Ophthalmol Vis Sci*. 1985; 26:1659–1694.
11. Flaxel CJ, Mulholland B, Haynes B, Gregor ZJ. Intraocular penetration of tamoxifen. *Ophthalmology*. 2000;107:2006–2009.
12. Toler SM. Oxidative stress plays an important role in the pathogenesis of drug-induced retinopathy. *Exp Biol Med (Maywood)*. 2004;229:607–615.
13. Bursch W, Ellinger A, Kienzl H, et al. Active cell death induced by the anti-estrogens tamoxifen and ICI 164 384 in human mammary carcinoma cells (MCF-7) in culture: the role of autophagy. *Carcinogenesis*. 1996;17:1595–1607.
14. Hwang JJ, Kim HN, Kim J, et al. Zinc(II) ion mediates tamoxifen-induced autophagy and cell death in MCF-7 breast cancer cell line. *Biometals*. 2010;23:997–1013.
15. Kelekar A. Autophagy. *Ann N YAcad Sci*. 2005;1066:259–271.
16. Tanida I, Ueno T, Kominami E. LC3 conjugation system in mammalian autophagy. *Int J Biochem Cell Biol*. 2004;36: 2503–2518.
17. Koh JY, Choi DW. Quantitative determination of glutamate mediated cortical neuronal injury in cell culture by lactate dehydrogenase efflux assay. *J Neurosci Methods*. 1987;20:83–90.
18. Kallio A, Zheng A, Dahllund J, Heiskanen KM, Härkönen P. Role of mitochondria in tamoxifen-induced rapid death of MCF-7 breast cancer cells. *Apoptosis*. 2005;10:1395–1410.
19. Hwang JJ, Lee SJ, Kim TY, Cho JH, Koh JY. Zinc and 4-hydroxy-2-nonenal mediate lysosomal membrane permeabilization induced by H2O2 in cultured hippocampal neurons. *J Neurosci*. 2008;28:3114–3122.
20. Lee SJ, Park MH, Kim HJ, Koh JY. Metallothionein-3 regulates lysosomal function in cultured astrocytes under both normal and oxidative conditions. *Glia*. 2010;58:1186–1196.
21. Thomas S, Thurn KT, Bicaku E, Marçhion DC, Műnster PN. Addition of a histone deacetylase inhibitor redirects tamoxifen-treated breast cancer cells into apoptosis, which is opposed by the induction of autophagy. *Breast Cancer Res Treat*. 2011;130:437–447.
22. Ma D, Tremblay P, Mahngar K, et al. A novel synthetic C-1 analogue of 7-deoxypancratistatin induces apoptosis in p53 positive and negative human colorectal cancer cells by targeting the mitochondria: enhancement of activity by tamoxifen. *Investig New Drugs*. 2011;453:145–158.
23. Bains M, Heidenreich KA. Live-cell imaging of autophagy induction and autophagosome-lysosome fusion in primary cultured neurons. *Methods Enzymol*. 2009;453:145–158.
24. Yoon YH, Cho KS, Hwang JJ, Lee SJ, Choi JA, Koh JY. Induction of lysosomal dilatation, arrested autophagy, and cell death by chloroquine in cultured ARPE-19 cells. *Invest Ophthalmol Vis Sci*. 2010;51:6030–6037.
25. Kim HN, Lee SJ, Koh JY. The neurosteroids, allopregnanolone and progesterone, induce autophagy in cultured astrocytes. *Neurochem Int*. 2011;60:125–133.
26. Bjrky G, Lamark T, Pankiv S, Øvervatn A, Brech A, Johansen T. Monitoring autophagic degradation of p62/SQSTM1. *Methods Enzymol*. 2009;452:181–197.
27. Dziedzic SA, Caplan AB. Autophagy proteins play cytoprotective and cytocidal roles in leucine starvation-induced cell death in Saccharomyces cerevisiae. *Autophagy*. 2012;8:731–738.
28. Moreau K, Luo S, Rubinsztein DC. Cytoprotective roles for autophagy. *Curr Opin Cell Biol*. 2010;22:206–211.
29. Hyrskyluoto A, Reijonen S, Kivinen J, Lindholm D, Korhonen L. GADD34 mediates cytoprotective autophagy in mutant huntingtin expressing cells via the mTOR pathway. *Exp Cell Res*. 2012;318:33–42.
30. Kaarniranta K. Autophagy–hot topic in AMD. *Acta Ophthalmol*. 2010;88:387–388.
31. Krohne TU, Stratmann NK, Kopitz J, Holz FG. Effects of lipid peroxidation products on lipofuscinogenesis and autophagy in human retinal pigment epithelial cells. *Exp Eye Res*. 2010;90: 465–471.
32. Traynor BJ, Bruijn L, Conwit R, et al. Neuroprotective agents for clinical trials in ALS: a systematic assessment. *Neurology*. 2006;67:20–27.
33. Chen S, Zhang X, Song L, Le W. Autophagy dysregulation in amyotrophic lateral sclerosis. *Brain Pathol*. 2012;22:110–116.
34. Lozano V, Serrano MA, Losada MJ, et al. Diagnostic and therapeutic challenges. *Retina*. 2007;27:1305–1310.
35. Mauget-Faÿsse M, Gambrelle J, Quaranta-El Maftouhi M. Optical coherence tomography in tamoxifen retinopathy. *Breast Cancer Res Treat*. 2006;99:117–118.
36. Geng Y, Kohli L, Klocke BJ, Roth KA. Chloroquine-induced autophagic vacuole accumulation and cell death in glioma cells is p53 independent. *Neuro Oncol*. 2010;12:473–481.
37. Fan S, Li L, Chen S, et al. Silibinin induced-autophagic and apoptotic death is associated with an increase in reactive oxygen and nitrogen species in HeLa cells. *Free Radic Res*. 2011;45:1307–1324.
38. Yu SW, Baek SH, Brennan RT, et al. Autophagic death of adult hippocampal neural stem cells following insulin withdrawal. *Stem Cells*. 2008;26:2602–2610.
39. Lee SJ, Koh JY. Roles of zinc and metallothionein-3 in oxidative stress-induced lysosomal dysfunction, cell death, and autophagy in neurons and astrocytes. *Mol Brain*. 2010;3:30.
40. Frazzini V, Rockabrand E, Mocchegiani E, Sensi SL. Oxidative stress and brain aging: is zinc the link? *Biogerontology*. 2006; 7:307–314.
41. Dineley KE, Votyakova TV, Reynolds IJ. Zinc inhibition of cellular energy production: implications for mitochondria and neurodegeneration. *J Neurochem*. 2003;85:563–570.
42. Rudolf E, Cervinka M. Zinc pyrithione induces cellular stress signaling and apoptosis in Hep-2 cervical tumor cells: the role of mitochondria and lysosomes. *Biometals*. 2010;23:339–354.
43. Yu H, Lou JR, Ding WQ. Clioquinol independently targets NF-kappaB and lysosome pathways in human cancer cells. *Anticancer Res*. 2010;30:2087–2092.
44. Chwieralski CE, Welte T, Bűhling F. Cathepsin-regulated apoptosis. *Apoptosis*. 2006;11:143–149.
45. Melo FR, Lundequist A, Calounova G, Wernersson S, Pejler G. Lysosomal membrane permeabilization induces cell death in human mast cells. *Scand J Immunol*. 2011;74:354–362.
46. Chen QY, Shi JG, Yao QH, et al. Lysosomal membrane permeabilization is involved in curcumin-induced apoptosis of A549 lung carcinoma cells. *Mol Cell Biochem*. 2012;359: 389–398.
47. Johansson AC, Appelqvist H, Nilsson C, Kågedal K, Roberg K, Ollinger K. Regulation of apoptosis-associated lysosomal membrane permeabilization. *Apoptosis*. 2010;15:527–540.
48. Zeng KW, Fu H, Liu GX, Wang XM. Aluminum maltolate induces primary rat astrocyte apoptosis via overactivation of the class III PI3K/Beclin 1-dependent autophagy signal. *Toxicol In Vitro*. 2012;26:215–220.
49. Zhang N, Chen Y, Jiang R, et al. PARP and RIP 1 are required for autophagy induced by 11′-deoxyverticillin A, which precedes caspase-dependent apoptosis. *Autophagy*. 2011;7: 598–612.
50. Han MH, Lee WS, Lu JN, et al. Tetraarsenic hexoxide induces beclin-1-induced autophagic cell death as well as caspase-dependent apoptosis in U937 human leukemic cells. *Evid Based Complement Alternat Med*. 2012;2012:201414.
51. Miki H, Uehara N, Kimura A, et al. Resveratrol induces apoptosis via ROS-triggered autophagy in human colon cancer cells. *Int J Oncol*. 2012;40:1020–1028.